

Flow Control of Non-Newtonian Fluid using Riga Plate: Reiner-Phillipoff and Powell-Eyring Viscosity Models

A. Ahmad

COMSATS University, Islamabad, Pakistan

†Corresponding Author Email: adeelahmed@comsats.edu.pk

(Received February 19, 2018; accepted July 28, 2018)

ABSTRACT

This article investigates the controlling effects of electromagnetic field generated by Riga plate on the boundary layer flow of non-Newtonian fluid. Two classical viscosity models of non-Newtonian fluids namely; Powell-Eyring and Reiner-Phillipoff fluid models have been considered to study the different behaviors of non-Newtonian fluid flow. Numerical solution of the problem in the presence of strong suction is obtained using the nonlinear shooting method. The results are studied in terms of modified Hartmann number, non-Newtonian fluid parameters and the Bingham number. Linear regression is performed on the numerical results to present the correlation expression for the skin friction.

Keywords: Riga plate; Non-Newtonian fluid; Flow control; Powell-Eyring; Reiner-Phillipoff; Correlation expression.

NOMENCLATURE

a	width of magnets and electrodes.	V_w	dimensionless suction velocity parameter.
B_m	Bingham number.	Z	modified Hartmann number.
\dot{j}_o	applied current density in the electrodes.	ρ_f	fluid density.
M_o	magnetization of the permanent magnets.	τ_{yx}	shear stress.
S	dimensionless deformation .	τ_s	reference shear stress.
(U, V)	velocity components in (X, Y) directions respectively	ω	dimensionless shear stress.
(u, v)	non-dimensional (x, y) velocity components.	μ	viscosity of the fluid.
U_w	velocity of the surface.	μ_o	zero-shear viscosity.
V_w	suction velocity at the surface.	μ_∞	upper Newtonian limiting viscosity.
		γ	dimensionless viscosity.

1. INTRODUCTION

The phenomenon of drag reduction (Singh 2004), which prevents the loss of mechanical energy, has been a topic of intensive research. Various methods have been proposed to reduce the drag in physical systems which include adding polymers in base fluid (Gyr *et al.* 1995), magnetic fields (Shatrov and Gerbeth 2007) and flexible walls (Zhao *et al.* 2004). Electromagnetic field is a useful agent for drag reduction and flow control in both electrically conducting fluids with weak conductivity like sea water and ionized gases as well as with strong conductivity like liquid metals. A fully contactless

control is possible solely by application of a magnetic field in the fluid with high electrical conductivity like liquid metal or semiconductor melt. Contrary to this, in the case of liquids with low conductivity, currents produced by externally applied magnetic fields are generally very low, even for magnetic fields of several Tesla (Gailitis and Lielausis 1961; Pantokartoras and Magyari 2009). External electric field must also be applied in order to achieve and maintain flow control. The capability of electro-magnetic field to affect fluid flow has been used since long with diverse degree of success (Gailitis and Lielausis 1961; Albrecht *et al.* 2006). Therefore, in order to compensate for the weak

electric field, it is necessary to apply an external electric field to attain an adequate flow control. To achieve the required generation of electric field along with magnetic field, a wall-parallel Lorentz force is generated by external electric and magnetic field. That force is able to alter the structure of a moving surface-driven boundary layer and stabilize its motion by slowing down its growth. Gailitis and Lielausis (1961) designed Riga plate to produce crossed magnetic and electric fields, which can generate a wall parallel Lorentz force in order to control the fluid flow. Riga plate comprises a distance wise lined up array of alternating electrodes and permanent magnets attached on a flat surface. Pantokratoras and Magyari (2009) examined the boundary layer flow over a horizontal Riga plate for the fluids with low electrical conductivity. In (Magyari and Pantokratoras 2011), they investigated the aiding and opposing effects of Lorentz force on the same problem. Pantokratoras (2011) studied Sakiadis and Blasius flow for Riga plate. Ahmad *et al.* (2016) examined the controlling behavior of Lorentz force in the presence of temperature fluxes and nanoparticles concentration. In another study Ahmad *et al.* (2017) studied the flow and heat transfer of Copper-water nanofluid with temperature dependent viscosity past a Riga plate.

The analysis of engineering problems involving transport phenomena of non-Newtonian fluid is far more complex as compared to one entailing the Newtonian fluids. Due to wide and frequent occurrence of non-Newtonian fluids in various applications in nature and technology, there has been considerable interest in the study of non-Newtonian fluids flow. Molten plastic, natural liquids like bloods, polymer solutions, varnishes, dyes, and suspensions are some non-Newtonian fluids to mention. Non-Newtonian fluid under apposite circumstances, displays dilatant, pseudoplastic, visco-elastic, visco-plastic and time-dependent behaviors. Power-law (Bird *et al.* 1987), Powell-Eyring (Yoon 1987), Reiner-Phillipoff (Na 1994), Carreau-Yasuda (Bird *et al.* 1987) and Ellis (Bird *et al.* 1987) fluids are some models of non-Newtonian fluid to mention. Among these empirical models Powell-Eyring and Reiner-Phillipoff fluids are of considerable importance. A few studies in literature have studied the flow of these fluids especially, Reiner-Phillipoff fluid (Ahmad 2016).

Bearing in mind the wide occurrence of non-Newtonian fluid in industry and limited consideration of above mentioned models for non-Newtonian fluid and application of Lorentz force due to Riga plate in flow control and drag reduction of weakly conducting fluid, this article is dedicated to study of flow control of non-Newtonian Reiner-Phillipoff and Powell-Eyring fluids using the electromagnetic field generated by a Riga plate.

2. PROBLEM DESCRIPTION

We consider the electro-magnetohydrodynamic (EMHD) boundary layer flow of a non-Newtonian fluid with weakly conduction over a moving

horizontal Riga plate with suction velocity V_o . The Riga plate consists of an alternating array of electrodes and permanent magnets mounted on a plane surface (see Fig. 1). The mathematical model governing the flow including the continuity and momentum equations is as follow:

$$\frac{\partial U}{\partial X} + \frac{\partial V}{\partial Y} = 0, \quad (1)$$

$$U \frac{\partial U}{\partial X} + V \frac{\partial U}{\partial Y} = \frac{\mu}{\rho_f} \frac{\partial \tau_{xy}}{\partial Y} + \frac{\pi j_o M_o}{8 \rho_f} \exp\left(-\frac{\pi}{a} y\right), \quad (2)$$

subject to the boundary conditions

$$U = U_w, V = V_w \text{ at } Y = 0, \quad (3)$$

$$U \rightarrow 0, \text{ as } Y \rightarrow \infty.$$

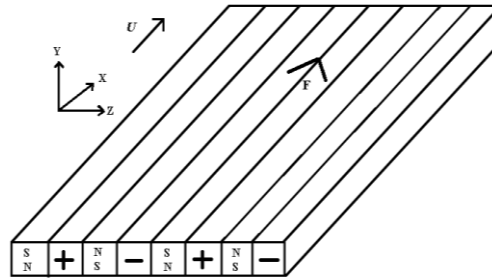


Fig. 1. Systematic diagram of Riga plate consisting the electrodes and magnets for the creation of an EMHD Lorentz force F in the flow along a flat plate.

In Eqs. (1)-(3), (U, V) are the velocity components in (X, Y) directions respectively, ρ_f is the fluid density and μ is the viscosity. j_o is the applied current density in the electrodes, M_o is the magnetization of the permanent magnets and a is the width of magnets and electrodes. Further, τ_{yx} is the shear stress, which is related to rate of strain non-linearly in different manner for different non-Newtonian fluids. For generality, we relate the shear stress and rate of strain by an arbitrary function as:

$$F\left(\tau_{yx}, \frac{\partial U}{\partial Y}\right) = 0. \quad (4)$$

We introduce the non-dimensional parameters

$$x = \frac{X}{l}, \quad y = \frac{Y}{L}, \quad u = \frac{U}{U_w}, \quad v = \frac{V}{V_o},$$

$$\omega = \frac{\tau_{yx}}{\tau_s}, \quad L = \frac{a}{\pi}, \quad l = \frac{U_w L^2}{\nu}, \quad V_o = \frac{\nu \pi}{a}$$

in equations (1)-(4) and obtain the dimensionless equations of the form

$$\frac{\partial u}{\partial x} + \frac{\partial v}{\partial y} = 0, \quad (5)$$

$$u \frac{\partial u}{\partial x} + v \frac{\partial u}{\partial y} = B_m \frac{\partial \omega}{\partial y} + Ze^{-y}, \quad (6)$$

$$F\left(\omega, \frac{\partial u}{\partial y}\right) = 0 \quad (7)$$

$$u = 1, v = v_w \text{ at } y = 0 \quad (8)$$

$$u(x, y) \rightarrow 0 \text{ as } y \rightarrow \infty.$$

where Z is the modified Hartmann number and B_m is the Bingham number given by the following expressions:

$$Z = \frac{1}{8\pi} \frac{a^2 j_o M_o}{v U_w \rho_f}, \quad B_m = \frac{a \tau_s}{\pi U_w \mu_\infty}.$$

With the supposition of strong suction (Pantokratoras 2008), continuity equation and condition $v = v_w$ at $y = 0$ implies $v = v_w$. Thus the governing equations may be written as:

$$v_w \frac{\partial u}{\partial y} = B_m \frac{\partial \omega}{\partial y} + Ze^{-y}, \quad (9)$$

$$F\left(\omega, \frac{\partial u}{\partial y}\right) = 0 \quad (10)$$

with associated boundary conditions

$$u = 1, \text{ at } y = 0, \quad (11)$$

$$u \rightarrow 0 \text{ as } y \rightarrow \infty.$$

Eq. (4) will have different forms for different models of non-Newtonian fluids. In this article, we will consider two empirical models namely; Reiner-Phillippoff and Powell-Eyring models for relating the shearing stress and deformation of the fluid.

2.1. Reiner-Phillippoff Fluid

For Reiner-Phillippoff fluid Eq. (4) i.e. stress deformation relationship gets the form:

$$\frac{\partial u}{\partial y} = \frac{\tau_{yx}}{\mu_\infty + \frac{\mu_o - \mu_\infty}{1 + \left(\frac{\tau_{yx}}{\tau_s}\right)^2}} \quad (12)$$

which is one of the classical descriptions of stress-deformation behavior (Na 1994; Ahmad 2016). In Eq. (12), τ_s is the reference shear stress. Actual liquids have Newtonian flow properties at relatively low and at very high shear rate. Correspondingly, μ_o is the zero-shear viscosity and μ_∞ is the upper Newtonian limiting viscosity. Reiner-Phillippoff model is one of a few non-Newtonian models which exhibit all the pseudoplastic, dilatant and Newtonian behaviors. In Eq. (12), the right hand side is known as flow function. The flow function in dimensionless form is given as:

$$f(\omega) = \frac{\omega}{1 + \frac{\lambda - 1}{1 + \omega^2}} \quad (13)$$

where $\omega = \tau_{yx} / \tau_s$ and $\lambda = \mu_o / \mu_\infty$. For $\lambda = 1$ we get Newtonian flow function. For $\lambda < 1$ Reiner-Phillippoff fluid behaves as dilatant fluid and pseudoplastic for $\lambda > 1$. The stability condition $df/d\omega > 0$ determines that λ must not exceed the critical value 9. In the case of Reiner-Phillippoff fluid Eq. (10) i.e. is relation between ω and $\frac{\partial u}{\partial y}$

may be written as:

$$\omega = \frac{1}{B_m} \frac{\partial u}{\partial y} \frac{\omega^2 + \lambda}{1 + \omega^2} \quad (14)$$

2.2. Powell-Eyring Fluid:

Despite of its mathematical complexity, Powell-Eyring fluid model is attended extensively by the researchers. This model stands superior as compared to other empirical models due to two reasons. Firstly, this model can be deduced from the kinetic theory of liquids rather than the empirical relation as in the case of other models like power law model. Secondly, it appropriately presents the Newtonian behavior for high and low shear rates where the power-law model shows an infinite effective viscosity for low shear rate which restrict its range of applicability.

The Powell Eyring model is based on Eyring reaction rate theory which gives it a strong thermodynamics foundation (Barth at al. 2008). This theory treats viscous diffusion as a ‘rate process’ described by a sum of exponential decay terms at the molecular level which leads to an expansion of the viscosity in terms of inverse hyperbolic sine function. Relating the first two terms in such an expansion leads to the 3-parameter Powell Eyring model:

$$\mu = \mu_\infty + (\mu_o - \mu_\infty) \frac{\sinh^{-1}\left(\lambda \frac{\partial U}{\partial Y}\right)}{\lambda \frac{\partial U}{\partial Y}}, \quad (15)$$

where μ_o is the limiting viscosity at the zero strain rate, μ_∞ is the limiting viscosity as $\frac{\partial U}{\partial Y} \rightarrow \infty$ and λ is the characteristic time. In dimensionless form, Eq. (15) can be written as:

$$\gamma = \frac{\mu_\infty}{\mu_o} + \left(1 - \frac{\mu_\infty}{\mu_o}\right) \frac{\sinh^{-1}(S)}{S}, \quad (16)$$

where $S = \lambda \frac{\partial U}{\partial Y}$ and $\gamma = \frac{\mu}{\mu_o}$ are dimensionless deformation and viscosity respectively.

Fig. 2 contains γ versus S curves for different values of fraction of limiting viscosities at zero and infinity strain. It is observed that in each case the viscosity is decreasing function of strain which depicts that Powell-Eyring model represents group of shear thinning fluids.

Using the Powell Eyring viscosity model (15), we get the following stress-strain relationship:

$$\tau_{yx} = \mu_\infty \frac{\partial U}{\partial Y} + \frac{\mu_o - \mu_\infty}{\lambda} \sinh^{-1} \left(\lambda \frac{\partial U}{\partial Y} \right). \quad (17)$$

Taking the second order approximation of the function:

$$\sinh^{-1} \left(\lambda \frac{\partial U}{\partial Y} \right) \cong \lambda \frac{\partial U}{\partial Y} - \frac{1}{6} \left(\lambda \frac{\partial U}{\partial Y} \right)^3, \quad (18)$$

$$\left| \lambda \frac{\partial U}{\partial Y} \right| \ll 1$$

Eq. (17) may be written as:

$$\tau_{yx} = \mu_\infty \frac{\partial U}{\partial Y} + \frac{\mu_o - \mu_\infty}{\lambda} \left(\lambda \frac{\partial U}{\partial Y} - \frac{1}{6} \left(\lambda \frac{\partial U}{\partial Y} \right)^3 \right), \quad (19)$$

$$\left| \lambda \frac{\partial U}{\partial Y} \right| \ll 1$$

In non-dimensional form the stress deformation relation may be written as:

$$\omega = \frac{1}{B_m} \left(\left(1 + \frac{1}{\alpha} \right) \frac{\partial u}{\partial y} - \frac{1}{6} \frac{\beta}{\alpha} \left(\frac{\partial u}{\partial y} \right)^3 \right), \quad (20)$$

where $\alpha = \frac{\mu_\infty / \mu_o}{1 - \mu_\infty / \mu_o}$ and $\beta = \left(\lambda \frac{U_w}{L} \right)^2$.

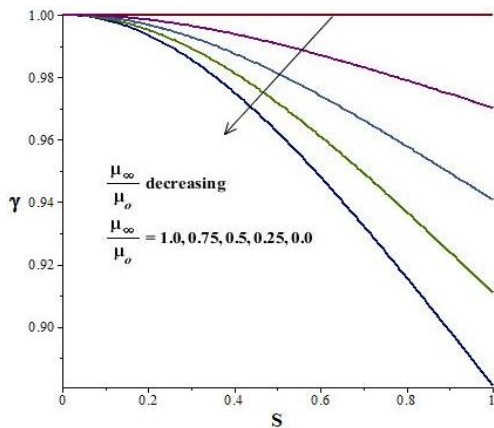


Fig. 2. Dimensionless viscosity verses dimensionless strain rate for Powell Eyring model.

3. Results and Discussion

One of the physical quantities of practical interest is skin friction coefficient which is defined as:

$$C_f = \frac{\tau_w}{\rho U_w^2}, \quad (21)$$

where τ_w is the shear stress at the surface. For Reiner-Phillippoff fluid τ_w may be expressed as:

$$\tau_w = \left(\mu_\infty + \frac{\mu_o - \mu_\infty}{1 + \left(\frac{\tau_w}{\tau_s} \right)^2} \right) \frac{\partial u}{\partial y} \Big|_{y=0}, \quad (22)$$

and for Powell-Eyring fluid we have

$$\tau_w = \mu_\infty \frac{\partial U}{\partial Y} + \frac{\mu_o - \mu_\infty}{\lambda} \left(\lambda \frac{\partial U}{\partial Y} - \frac{1}{6} \left(\lambda \frac{\partial U}{\partial Y} \right)^3 \right) \Big|_{Y=0}. \quad (23)$$

Using expressions (22) and (23) in (21), the skin friction coefficient for Reiner-Phillippoff fluid may be written as:

$$C_f \text{ Re} = \left(\frac{\omega^2 + \lambda \frac{\partial u}{\partial y}}{1 + \omega^2} \right) \Big|_{y=0},$$

and for Powell Eyring fluid it has the expression

$$C_f \text{ Re} = \left(\left(1 + \frac{1}{\alpha} \right) \frac{\partial u}{\partial y} - \frac{1}{6} \frac{\beta}{\alpha} \left(\frac{\partial u}{\partial y} \right)^3 \right) \Big|_{y=0}.$$

In this section we discuss the effects of Riga plate on the flow of non-Newtonian fluid with different stress strain relationships. The numerical solutions of the boundary value problem (9)-(11) with stress deformation relationships (14) and (20) for Reiner-Phillippoff fluid and Powell-Eyring fluid respectively are obtained, using nonlinear shooting method. Anon linear regression is executed on the numerical results to write the correlation expressions for skin friction.

Firstly, we discuss the Reiner-Phillippoff fluid model. In Table 1, some correlation of skin friction for different values of Bingham number B_m and suction parameter s are presented with corresponding maximum percentage error. It is observed from these expressions that the rate of change of skin friction with respect to λ is very small. Resultantly, we only discuss the effect of Bingham number and modified Hartmann number on the skin friction graphically.

In Fig. 3, the behavior of skin friction for Reiner-Phillippoff fluid over a Riga plate is plotted. It is mentioned that Lorentz force can play an important role in controlling the skin friction. In (Magyari and Pantokratoras 2011), it is mentioned that the Lorentz force due to the Riga plate play flow aiding role for $Z > 0$ and opposing role for $Z < 0$ and it is observed that as Z increases, the assisting role of Lorentz force increases causing an increase in flow velocity. Ultimately, an increase in modified Hartmann number also increases the skin friction. The same behavior can be observed from the correlation expression for the skin friction i.e. the rate of change of skin friction with respect to modified Hartmann number (C_Z) is positive. Another important observation from Table 1 and Fig. 3 is that the rate of change of skin friction with respect to modified Hartmann number is much higher for small Bingham number as compared to large Bingham number.

Table 1 Correlation of skin friction coefficient ($ReC_f=C + C_\lambda\lambda + C_ZZ$) of Reiner-Phillippoff fluid with maximum percentage error for different values of Bingham number and suction parameter where the values of Z is considered in the interval $(-2, 3)$ and λ in the interval $(0, 5)$

B_m	S	C	C_λ	C_Z	Max. % error
0.1	2.0	-19.998	-0.005	9.990	Less than 1 %
1.0	2.0	-1.995	-0.003	0.998	Less than 1 %
2.0	2.0	-0.997	0.002	0.499	Less than 1 %

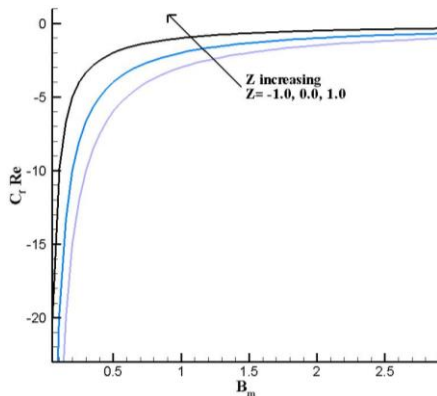


Fig. 3. Behavior of skin friction for Reiner-Phillippoff fluid over a Riga plate for $\lambda=3.0$ and $s=2.0$.

In Figs. 4 and 5, the effect of varying Bingham number on the flow velocity of pseudoplastic and dilatant fluids is presented respectively. It is observed that the velocity of the pseudoplastic fluid increases with an increase in Bingham number since a higher Bingham number represents a fluid that start flowing under higher shear stress ultimately possesses higher velocity. An opposite effect of Bingham number on the velocity of dilatant fluid is noticed. Since the dilatant fluids become thicker when agitated so the lower shear stress is more favorable for dilatant fluid to flow. So a dilatant fluid with lower Bingham number i.e. lower minimum stress required to flow would have a higher velocity.

In Fig. 6 the velocity profile of Powell-Eyring fluid as compare to viscous fluid in the presence of assisting and opposing Lorentz force and in the absence of Lorentz force is plotted. It is observed that the velocity of the fluid decreases as the fluid parameter $1/\alpha$ i.e. the effect of non-Newtonality increases. Besides the fact, the velocity of the fluid decreases as Z decreases due to assisting/ opposing role of the Lorentz force, it is further observed that the decrease in velocity due to presence of opposing effect of Lorentz force ($Z<0$) is more in non-Newtonian fluid as compare to Newtonian fluid and increase in velocity due to assisting role of Lorentz force in non-Newtonian fluid is less than the Newtonian fluid. Further the magnitude of rate of change of velocity with respect to y increase as $1/\alpha$ increases and Z decreases.

In Fig. 7 the velocity profile of Powell-Eyring fluid

for varying β in the presence and absence of assisting/opposing Lorentz force is plotted. It is observed that the velocity of the fluid decreases as the fluid parameter β increases. It is also observed that the magnitude of decrease in velocity due to varying β increases as we replace assisting Lorentz force with opposing Lorentz force.

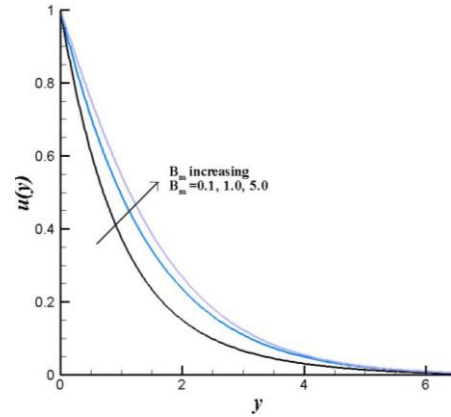


Fig. 4. Velocity profile of pseudoplastic Reiner-Phillippoff fluid ($\lambda>1$) for varying Bingham number B_m for $Z=1.0$, $v_w=-2.0$ and $\lambda=2.0$.

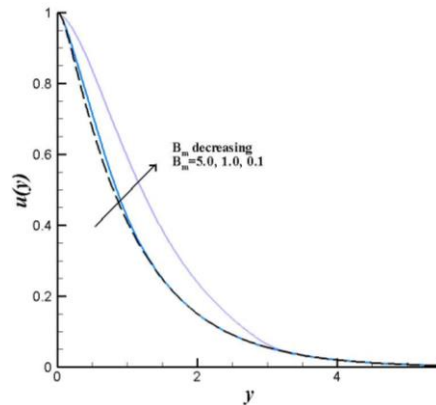


Fig. 5. Velocity profile of dilatant Reiner-Phillippoff fluid ($\lambda<1$) for varying Bingham number B_m for $Z=1.0$, $v_w=-2.0$ and $\lambda=0.5$.

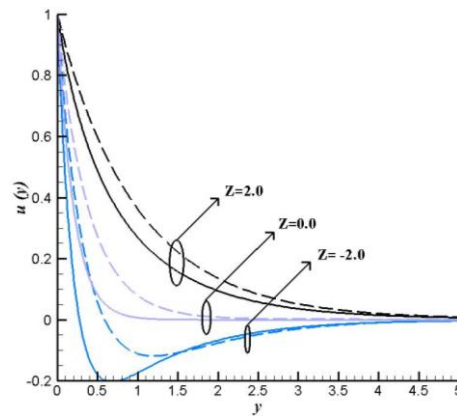


Fig. 6. Velocity profile of Powell-Eyring fluid for varying Z and $1/\alpha$ with $\beta=0.2$ and $v_m=-5.0$. Dashed curves are for $1/\alpha=0.0$ and solid curves are for $1/\alpha=1.0$.

In Table 2 the correlation expression for the skin friction of Powell-Eyring fluid is given for different values of fluid material parameter $1/\alpha$ and fixed value of suction parameter s . Each of the correlation expression is obtained by performing linear regression on 615 set of numerical values of skin friction for different β and Z .

Table 2 Correlation of skin friction coefficient ($Re_C = C + C_\beta\beta + C_Z Z$) of Powell-Eyring fluid with maximum percentage error for different values of $1/\alpha$ where the values of Z is considered in the interval $(-2, 2)$ and β in the interval $(0.0, 0.7)$ and $s = 5.0$

$1/\alpha$	C	C_β	C_Z	Max. % error
0.0	-5.0	0.0	1.0	0.001 %
0.01	-4.947	-0.262	1.038	3.344%
0.02	-4.884	-0.586	1.089	6.712 %
5.0	-0.828	-0.135	0.192	6.334 %
10.0	-0.457	-0.018	0.094	6.055%

In Fig. 8 skin friction is plotted for different involved parameters to conduct a comparative study of Powell-Eyring fluid with Newtonian fluid in the absence and presence of Lorentz force due to Riga plate. It is observe that the magnitude of skin friction is higher for higher modified Hartmann number Z . This is because of the assisting and opposing effects of Lorentz force. We can observe the value of skin friction for Newtonian fluid at $1/\alpha=0$. The skin friction for Powell- Eyring fluid increases as the value of $1/\alpha$ increase.

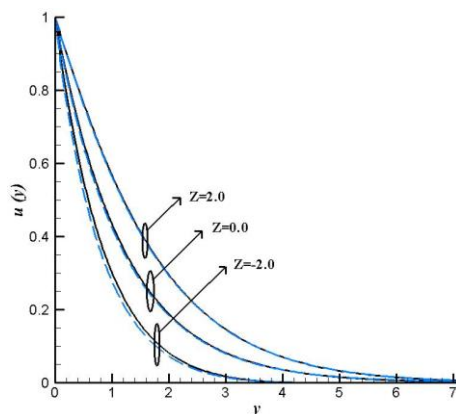


Fig. 7. Velocity profile of Powell-Eyring fluid for varying Z and β with $1/\alpha = 5.0$ and $vm = -5.0$. Dashed curves are for $\beta = 0.6$ and solid curves are for $\beta = 0.0$.

Further the rate of change in skin friction with respect to $1/\alpha$ in the presence of Lorentz force is different as compare to in the absence of Lorentz force. It decrease in the presence of assisting Lorentz force and increases in the presence of opposing Lorentz force. Further the skin friction decreases

with an increase in parameter β . This change in skin friction with respect to β becomes negligible for larger values of $1/\alpha$. The last two observations can also be seen from table 2. An important phenomena observed from Table 2 is that the magnitude of rate of change with respect to Z and β (magnitude of C_Z and C_β respectively) increases for $1/\alpha < 1$ and decreases for $1/\alpha > 1$. This fact can also be observed if we closely examine the Fig. 8.

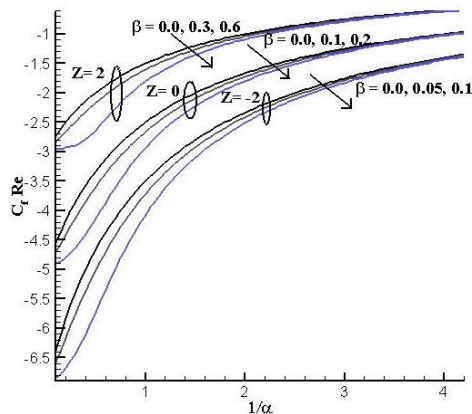


Fig. 8. Skin friction of Powell-Eyring fluid for varying involved parameters.

4. CONCLUSION

In this article, we considered two empirical models of non-Newtonian fluids to examine the controlling effects of Lorentz force due to cross electric and magnetic fields generated by a Riga plate. The mathematical model incorporating the Grinberg-term for the wall parallel Lorentz force due to Riga plate is solved numerically. The correlation expressions for skin friction are also developed by performing linear regression on the obtained numerical data to provide the readers with the analytical expression for further investigation. Some important observations are as follow:

1. For Reiner-Phillippoff fluid model, the rate of change of skin friction with respect to modified Hartmann number is much higher for small Bingham number as compared to large Bingham number. The velocity of the pseudoplastic fluid increases with an increase in Bingham number and an opposite effect is noticed for dilatant fluid.
2. For Powell-Eyring fluid model, the rate of change of skin friction with respect to $1/\alpha$ decrease in the presence of assisting Lorentz force and increases in the presence of opposing Lorentz force. Further, the skin friction decreases with an increase in parameter β and becomes negligible for larger values of $1/\alpha$.

REFERENCES

Ahmad, A. (2016). Flow of Reiner–Phillippoff based nano-fluid past a stretching sheet. *J. Mol. Liq.*.

- 219, 643–646.
- Ahmad, A., S. Ahmed and F. M. Abbasi (2017). Flow and Heat Transfer Analysis of Copper-water Nanofluid with Temperature Dependent Viscosity Past a Riga Plate. *Journal of Magnetism*. 22(2), 181-187.
- Ahmad, A., S. Asghar and S. Afzal (2016). Flow of nanofluid past a Riga plate. *Journal of Magnetism and Magnetic Materials*. 402, 44–48
- Albrecht, T., R. Grundmann, G. Mutschke and G. Gerbeth (2006). Electromagnetic control of a transitional boundary layer. Fifth International Conference on CFD in the Process Industries CSIRO, Melbourne, Australia.
- Barth, W. L., L. V. Branets and G. F. Carey (2008). Non-Newtonian flow in branched pipes and artery models. *Int. J. Numer. Meth. Fluids*. 57, 531–553.
- Bird, R. B., R. C. Armstrong and O. Hassager (1987). *Dynamics of polymeric liquids Vol. 1*, Wiley, New York, USA.
- Gailitis, A. and O. Lielausis (1961). On a possibility to reduce the hydrodynamic resistance of a plate in an electrolyte. *Appl. Magneto hydro dyn.* 12, 143–146.
- Gyr, A., H. W. Bewersdorff and Kluwer (1995). *Drag Reduction of Turbulent Flow by Additives*, Academic Publishers, Dordrecht.
- Magyari, E. and A. Pantokratoras (2011). Aiding and opposing mixed convection flows over the Riga plate. *Commun. Nonlinear Sci. Numer. Simulat.* 16, 3158–3167.
- Na, T. Y. (1994). Boundary Layer Flow of Reiner-philippoff Fluids. *Int. J. Non-Lluw Mechanics*. 29(6), 871477.
- Pantokratoras, A. (2008). Some exact solutions of boundary layer flows along a vertical plate with buoyancy forces combined with Lorentz forces under uniform suction. *Mathematical Problems in Engineering*. 18, 149272.
- Pantokratoras, A. (2011). The Blasius and Sakiadis flow along a Riga plate. *Prog. Comput. Fluid Dyn.* 11(5), 329–333.
- Pantokratoras, A. and E. Magyari (2009). EMHD free-convection boundary-layer flow from a Riga plate. *J. Eng. Math.* 64, 303–315.
- Shatrov, V. and G. Gerbeth (2007). Magneto-hydrodynamic drag reduction and its efficiency. *Physics of Fluids*. 19(3), 035109.
- Singh, R. P. (2004). Drag Reduction. *Encyclopedia of Polymer Science and Technology*.
- Yoon, H. K. (1987). A note on the Powell-Eyring fluid model. *Int. Comm. Heat Mass Transfer*. 14, 381-390.
- Zhao, H., J. Z. Wu and J. S. Luo (2004). Turbulent drag reduction by traveling wave of flexible wall. *Fluid Dyn. Res.* 34, 175–198.